JGR Space Physics

RESEARCH ARTICLE
10.1029/2019JA026853

Isolated Auroral Spots Observed by DMSP/SSUSI

Su Zhou[1], Xiaoli Luan[2], Viviane Pierrard[3], and Desheng Han[1]

[1]State Key Laboratory of Marine Geology, School of Ocean and Earth Science, Tongji University, Shanghai, China, [2]CAS Key Laboratory of Geospace Environment, School of Earth and Space Sciences, University of Science and Technology of China, Hefei, China, [3]Royal Belgian Institute for Space Aeronomy, Brussels, Belgium

Key Points:
- The isolated auroral spots were produced predominantly by energetic ions (10–240 keV) and electrons (30–300 keV)
- The isolated auroral spots corotated with the Earth and lasted for ~10 hr
- The energetic ions related to the auroral spots were likely scattered by the EMIC waves and were mapped in the vicinity of the plasmapause

Supporting Information:
- Supporting Information S1

Correspondence to:
X. Luan,
luanxl@ustc.edu.cn

Citation:
Zhou, S., Luan, X., Pierrard, V., & Han, D. (2019). Isolated auroral spots observed by DMSP/SSUSI. *Journal of Geophysical Research: Space Physics*, *124*, 8416–8426. https://doi.org/10.1029/2019JA026853

Received 16 APR 2019
Accepted 8 SEP 2019
Accepted article online 12 OCT 2019
Published online 6 NOV 2019

Abstract This work reports auroral spots event observed by the SSUSI instruments on board the DMSP spacecraft between 22 and 23 July 2009 during the recovery phase of a moderate magnetic storm. The spots were observed between 18:00 and 02:00 magnetic local time and stayed at ~60° magnetic latitude. They lasted for ~10 hr and corotated with ~64% of the Earth's rotational speed. In situ observations indicate that the isolated auroral spots were produced by energetic ions at energies between 10 and 240 keV, with significantly anisotropic electron (30–300 keV) precipitations. It is expected that the energetic ions originate from the ring current and can be scattered by the EMIC waves through cyclotron resonance. The energetic electrons can be precipitated by the nonresonant interaction between the electrons and EMIC waves, which is suggested by previous works.

1. Introduction

Since detached arcs and auroral patches were first reported by Moshupi et al. (1979), they have been the focus of much attention. Detached arcs and auroral patches are isolated equatorward from the auroral oval (Moshupi et al., 1979). Detached arcs are mostly observed in the afternoon sector during geomagnetic storm recovery phase and the corresponding geomagnetic activity is mostly weak (Burch et al., 2002; Immel et al., 2002; Mendillo et al., 1989; Moshupi et al., 1979). Previous investigations have indicated that the afternoon detached arcs can be mapped to the plasmaspheric plume location that overlaps with the ring current (Spasojević et al., 2004). Recent studies suggested that the afternoon detached arcs were created by the ring current ions presumed to be scattered into the loss cone by electromagnetic ion cyclotron (EMIC) waves (Yuan et al., 2010).

Detached arcs are often observed in a constant magnetic local time (MLT) sector indicating a westward moving with respect to the Earth (Frey, 2007). However, auroral patches were found to corotate with the Earth (Moshupi et al., 1979). Frey et al. (2004) have used the IMAGE spacecraft to investigate subauroral morning proton spots (SAMPS) that rotated with 70–95% of the Earth's rotation speed. The coincident particle spectra measured by DMSP indicated source to be pure ions with mean energies above 30 keV (Frey et al., 2004). Similar subauroral proton spots were also observed in the duskside by the IMAGE spacecraft, and were suggested to have a good agreement with Pc1 (0.2–5 Hz) pulsation (Yahnin et al., 2007). Sakaguchi et al. (2008) have used an all-sky imager to report several isolated auroral arcs in both the premidnight and postmidnight sectors. These isolated auroras appeared to be arcs instead of spots, and the sectors in which the arcs were observed were different from the SAMPS (Frey et al., 2004) and subauroral proton spots (Yahnin et al., 2007). The coincident particle data and magnetometer measurement indicated that the isolated auroral arcs can be created by 30–250-keV ions scattered by He^+ EMIC waves (Sakaguchi et al., 2008). Another study showed the coincident precipitation of ions with energies of tens of keV and precipitation of relativistic electrons into an isolated proton aurora (Miyoshi et al., 2008). Kubota et al. (2003) reported evening corotating patches (ECP) observed by the all-sky imaging system in Alaska. The ECPs were observed around 65.5° MLAT and between 16 and 19 MLT during a geomagnetically quiet period, lasting for more than 40 min. They suggested that the ECP auroras were created by precipitating electrons with energies greater than several keV (Kubota et al., 2003). Mendillo et al. (1989) used ground-based all-sky imagers to investigate isolated patches which were very likely produced by energetic ions with energies above 10 keV.

Mostly the isolated spots or patches mentioned above were observed during the recovery phases of magnetic storms. Zhang et al. (2005) have reported some nightside detached auroras (NDAs) observed by TIMED/GUVI during intense magnetic storms. The NDAs appeared to be thin arcs likely due

to soft (<1 keV) ion precipitation, or to be patches mostly created by energetic (~10 keV) precipitating ions.

Up to now, most investigations focus on the isolated auroral arcs or spots created by energetic ions. In this paper, we perform an analysis of isolated auroral spots, which are not only associated with energetic ions, but also energetic electrons. In addition, these spots are long-lasting and appear to corotate with the Earth. We will report this interesting aurora case using various instruments and discuss the possible wave-particle interaction mechanisms. In the next section, we shall give a brief introduction to the instrumentation. The observations will be shown in section 3. We will give a detailed discussion in section 4 and a brief summary in section 5, respectively.

2. Instrument and Data

2.1. DMSP/SSUSI

The Special Sensor Ultraviolet Spectrographic Imager (SSUSI) is a far-ultraviolet (FUV) imager on board the Defense Meteorological Satellite Program (DMSP) spacecraft (Paxton et al., 2002). The DMSP includes a series of satellites operating at an altitude of ~840 km. The DMSP satellites are Sun-synchronous, polar orbiting around the Earth. The inclination of the satellites is ~98.9° and the period is ~101 min (Hardy et al., 1984). DMSP F16 and F17 were launched on 18 October 2003 and 4 November 2006, respectively. The first SSUSI was mounted on DMSP F16 satellite. SSUSI observes FUV spectrum in five bands: HI Lyman α (121.6 nm), OI (130.4 nm), OI (135.6 nm), N_2 LBHS (140–160 nm), and N_2 LBHL (160–180 nm; Paxton et al., 2002; Sotirelis et al., 2013). The SSUSI contains a scanning imaging spectrograph (SIS) that scans the FUV spectrum perpendicular to the spacecraft track. Each scanning image is a built up over 20–30 min when the satellite flies over the polar region. In this work, the "average UT time" for each image is referred to the median UT. We use the N2 LBHS emission which is mostly produced by precipitating electrons and secondary electrons produced by protons.

2.2. DMSP/SSJ

The Special Sensor J (SSJ) mounted on the DMSP is intended to monitor the precipitating ions and electrons that cause auroras at high latitude (Hardy et al., 1984). SSJ/4 on board DMSP F16-F15 measures the energy flux of ions and electrons at energies ranging from 30 eV to 30 keV separated into 19 logarithmical energy channels (Hardy et al., 1984; Redmon et al., 2017). These SSJ/4 sensors have a field of view (FOV) lower than 12°. These sensors point toward zenith direction and measure the precipitating electrons and ions in the loss cone. SSJ/5 sensors were mounted on DMSP F16 and beyond. The energy range and energy channels for the sensors were designed to match SSJ/4. Each SSJ/5 sensor contains a spherical electrostatic analyzer that provides six nonoverlapping in-plane look directions with 4° × 15° for each direction. The total field of view is 4° × 90° (Redmon et al., 2017). This 90° total FOV covers the ram direction to zenith.

2.3. POES

The particle data observed by the Polar Orbiting Environment Satellites (POES) will also be used in this work. POES 16 was launched to a Sun-synchronous orbit in September 2000. The spacecraft orbit altitude is ~830 km with an orbit period of 102 min. The Medium Energy Proton and Electron Detector (MEPED), on board POES, consists of two directional electron telescopes and two directional proton telescopes (Evans & Greer, 2000). One telescope points radially upward, called the 0° detector which measures particles in the loss cone at high latitudes. Another telescope is called the 90° detector which detects particles with a small portion in the loss cone and perpendicular to the first one. The field of view of both detectors is 30° (Evans & Greer, 2000). The proton energy range observed by MEPED is divided into six differential channels ranging from 30 to more than 6,900 keV. The electron energy range contains three integrated energy channels >30, >100, and >300 keV.

2.4. Solar Wind Data and CARISMA Magnetometers

The solar wind data used in the present study were obtained from OMNI with temporal resolution of 1 min. These solar wind parameters have been time shifted to the bow shock of the Earth (King & Papitashvili, 2005). In addition, we will use the magnetic field data obtained at ground stations to investigate EMIC wave along with subauroral spots. The Canadian Array for Realtime Investigations of Magnetic Activity

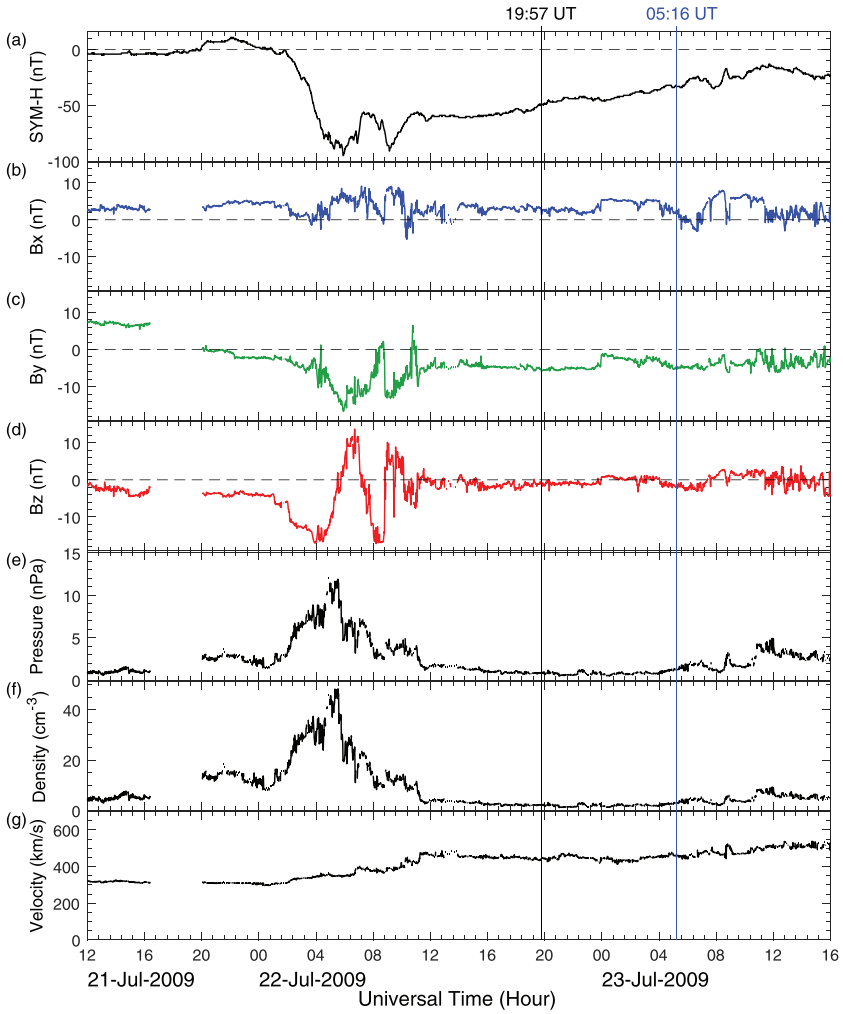

Figure 1. (a) *SYM-H*, (b) IMF B_x, (c) IMF B_y, (d) IMF B_z, (e) solar wind dynamic pressure, (f) solar wind density, and (g) solar wind bulk velocity between 12:00 UT on 21 July 2009 and 16:00 UT on 23 July 2009. The two vertical lines indicate the time interval of the isolated auroral spots as shown in Figure 2.

(CARISMA) is an array of magnetometers that are used to measure disturbances in the Earth's magnetic field driven by the magnetosphere-solar wind coupling. In this study, we employ the magnetometer data from the PINA station (MLAT = 59.98°, MLON = 331.75°) with a resolution of 8 Hz (Mann et al., 2008).

3. Observations

A moderate magnetic storm took place on 22 July 2009 with a minimum *SYM-H* index of −90 nT. Figure 1 gives the geomagnetic indices and the corresponding solar wind plasma parameters. Figure 1a shows that the *SYM-H* index reached a minimum of −90 nT at 06 universal time (UT) on 22 July 2009. The *SYM-H* increased to −60 nT, and decreased to −90 nT again at 09 UT due to the northward turning in IMF B_z as shown in Figure 1d. Then the magnetic storm began its recovery phase.

3.1. DMSP/SSUSI Observations

During the late recovery phase of the magnetic storm, the SSUSI on board DMSP F16 and F17 observed isolated spots at subauroral latitudes in the southern hemisphere from 22 to 23 July 2009. The SSUSI images are shown in Figure 2, and the auroral spots are indicated by gray arrows. The red lines indicate footprints of the DMSP spacecraft, with arrows indicating flying directions. Because of the 98.8° inclination of the orbit and the offset between the geomagnetic and geographic axes, in MLT-MLAT coordinates the spacecraft scanning images are located in the nightside in the southern hemisphere and in the dayside in the northern

hemisphere. Therefore, only images in the southern hemisphere are shown in Figure 2. It is clear to see in Figure 2b that an auroral spot was observed by DMSP F17/SSUSI at 19:57 UT in the evening sector. It is detached from the main auroral oval and located around 18:50 MLT and at 60° MLAT. The corresponding solar wind plasma parameters are stable as indicated by the vertical black line in Figure 1. Figure 2c shows that the spot was observed by DMSP F16/SSUSI at 20:52 UT with a clearly eastward shift with respect to the one in Figure 2b. It is therefore expected that the auroral spot corotated with the Earth. As shown by the gray arrow in Figure 2d, three auroral spots were observed around 21:37 UT. The spot in the east side of Figure 2d likely corresponds to the spot in Figure 2c due to the characteristic of "corotation." Figures 2e and 2f indicate that the auroral spots disappeared for nearly 3 hr. However, Figures 2g–2j show that they occurred again and moved toward the midnight sector. The auroral spots in Figure 2j moved eastward significantly with respect to those in Figure 2g, and they had similar morphologies of spots. It is therefore reasonable to conclude that the auroral spots corotated with the Earth.

3.2. In Situ Observations

In order to investigate the precipitating particles creating the auroral spots as mentioned above, Figure 3 gives the particle measurements of DMSP F16 corresponding to the spots in Figure 2c. As shown in Figure 3d, the isolated spots were produced by strong precipitating ions at energies above 10 keV. Figure 3c also shows an enhancement in the electron energy flux corresponding to the auroral spots, but its intensity was small and was just slightly above the background noise. Since DMSP failed to measure particles at energies above 30 keV, the ion energies associated with the auroral spots were possibly greater than 30 keV.

Figure 4 gives the particle measurements of POES 16 between 21:40 and 21:50 UT on 22 July 2009. The POES track during this time interval was indicated by a blue line in Figure 2d. The black box in Figure 4 denotes the precipitating particles observed around 18:35 MLT and 21:46:30 UT. It is worthwhile to note that the spot in the west side of Figure 2d was located around 18:24 MLT at 21:37 UT. This spot was expected to move to 18:35 MLT in 9 min (the corotating speed of the spots will be discussed later), and then it was observed by POES 16 spacecraft around 21:46:30 UT. Figures 4a and 4b show the precipitating ions with energy between 30 and 240 keV into the isolated auroral spots. This result is not contradictory with the DMSP in situ observations as shown in Figure 3, since the DMSP/SSJ is not able to measure particles with energy above 30 keV. Figure 4c also shows an increase in the energy flux of protons with energy between 240 and 800 keV, which was less than the flux of the protons with energies between 30 and 240 keV. Figures 4d–4f give the observations of precipitating electrons above 30 keV corresponding to the auroral spots. The three panels indicate that the isolated spots were related to an enhancement in the electron energy flux above 30 keV. It is interesting to note that the enhancement in the electron energy flux was most significant for >30 keV, less obvious for >100 keV, and less significant for >300 keV. This result implies that the electrons at energies between 30 and 300 keV precipitate into the isolated spots.

3.3. Pc1 Associated With the Isolated Auroral Spots

Based on the images shown in Figure 2, the locations of the auroral spots are used to determine their corotation speed. Figure 5a gives the MLT of the eastside edge of the auroral spots as a function of UT. The result suggests that the occurrence locations of the spots can be fitted well by a straight line, with a correlation coefficient of 0.99 between the spot locations and occurrence UT time. This result indicates that the auroral spots shown in Figures 2b–2d and 2g–2k are likely to be the same event. The slope of the fitted line gives 64% of the full corotation speed of the Earth.

In order to investigate the mechanism causing the energetic particles to be precipitated, we use magnetometer data to study the geomagnetic pulsations. The PINA station in the northern hemisphere contains a magnetometer to measure the magnetic field perturbations with eight samples per second. Figure 5b displays the estimated locations of the auroral spots and PINA station at 02:30 UT on 23 July 2009. The locations of the auroral spots are calculated from the spot corotating speed indicated by the fitted line in Figure 5a. At 02:30 UT on 23 July 2009, the PINA station was near to the occurrence locations of the auroral spots. Figure 5c gives the Pc1 data between 00:00 UT and 12:00 UT on 23 July 2009. Pc1 observed at ground stations has been suggested to be caused by EMIC wave originating from the magnetosphere (Engebretson et al., 2008). Figure 5c shows three intense Pc1 pulsations between 01:00 and 08:00 UT, when the isolated auroral spots were also observed by the SSUSI instruments as shown in Figures 2g–2k. The frequency of the Pc1 is approximately equal to the

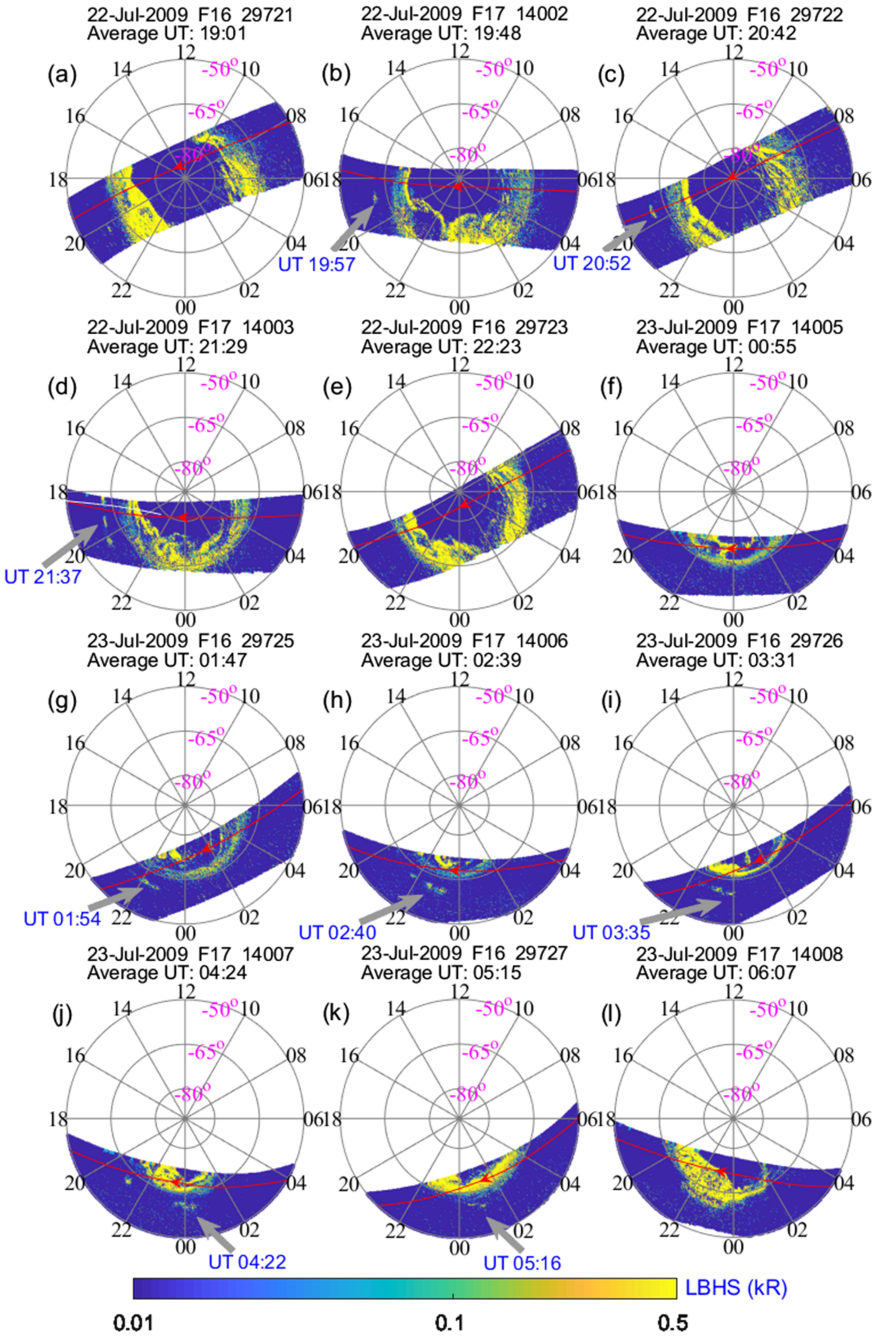

Figure 2. LBHS images observed by DMPS F16 and F17/SSUSI in the southern hemisphere on 22 and 23 July 2009. The data are mapped onto the geomagnetic coordinate with noon at the top of each panel. The spacecraft moved from the dawnside to duskside with red lines indicating spacecraft orbits. The average UT for each flight period is also given on the top. The auroral spots are indicated by gray arrows, and the corresponding UT is also given. A white line in (d) indicates the footprint of POES 16 between 20:40 and 21:50 UT on 22 July 2009.

gyrofrequency of Helium ion after 06:00 UT. Energetic protons are mostly injected at nightside and are presumed to be scattered into the loss cone at the equatorial plane. These protons can be precipitated in both hemispheres. It is worth noting that the PINA station is in the northern hemisphere, and the auroral spots were observed by the SSUSI in the southern hemisphere as shown in Figure 2. Since the DMSP orbit track shifts to the dayside in the northern hemisphere, only one image with auroral spots was observed by DMSP F16/SSUSI around 21:28 UT in the northern hemisphere (see Figure S1 in auxiliary materials).

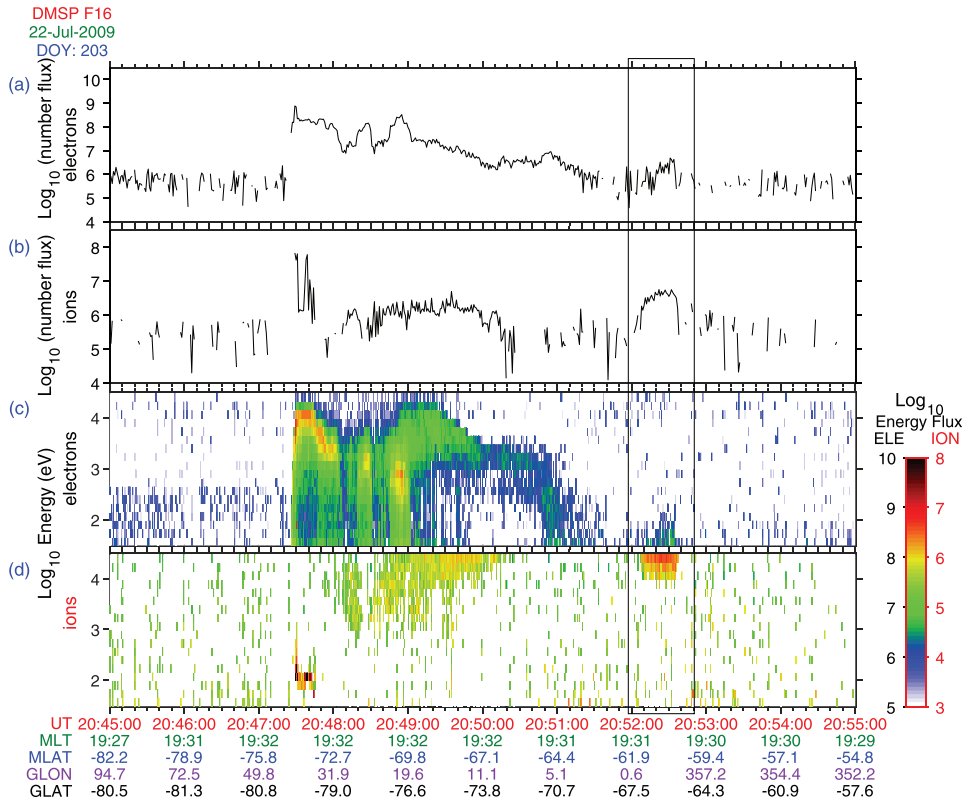

Figure 3. The particle data obtained from the DMSP/SSJ observations corresponding to Figure 2c. (a) Number flux of electrons in unit of #/(s cm^2 str), (b) number flux of ions in unit of #/(s cm^2 str), (c) differential energy flux for electrons in unit of eV/(s cm^2 str eV), and (d) differential energy flux for ions in unit of eV/(s cm^2 str eV). UT, geographic, and geomagnetic coordinates are given at the bottom. The black box indicates the time of the isolated auroral spots in Figure 2c.

4. Discussion

4.1. Particles Producing Isolated Auroral Spots

The isolated auroral spots have been observed by DMSP F16/SSUSI and F17/SSUSI in the southern hemisphere from 22 to 23 July 2009. They were observed in the evening sector between 18:00 and 02:00 MLT. They were stable in geomagnetic latitude and lasted for nearly 10 hr. The isolated spots corotated with 64% of the full speed of the Earth. Previous works have reported subauroral proton spots (Frey et al., 2004; Yahnin et al., 2007) observed by the IMAGE spacecraft and isolated auroral arcs (Sakaguchi et al., 2007) observed by all-sky imagers. Those auroral spots or arcs were mostly observed during the recovery phases of magnetic storms, and were suggested to be produced by energetic ring current ions (Frey et al., 2004; Sakaguchi et al., 2008; Yahnin et al., 2007). Mendillo et al. (1989) have reported auroral patches, which were suggested to be generated mainly by precipitating ions above ~10 keV via the measurements of the DMSP spacecraft. Up to now, very rare works focus on isolated spots in relation with ion and electron precipitations simultaneously. Miyoshi et al. (2008) have shown the ions with energies of tens of keV and MeV electrons into an isolated proton aurora. Zhang et al. (2005) have reported nightside detached auroras due to soft ion (<1 keV) or energetic ion (around 10 keV) precipitations during the development of major magnetic storms. However, it is not clear whether the detached auroras in their study corotated with the Earth. In the present work, the isolated auroral spots looked more like the subauroral protons spots (Frey et al., 2004; Yahnin et al., 2007) or auroral patches (Mendillo et al., 1989) based on their appearances and the characteristic of "corotation." These isolated auroral spots are found to be produced by energetic ions from 10 to 800 keV and electrons above 30 keV. Such energetic ions likely originate from the ring current which is expected to be filled with hot ions during the recovery phase of magnetic storms. The significantly precipitating electrons with energies between 30 and 300 keV are also observed into the isolated spots. Their energies are much less than MeV, thus unlikely to be scattered by the EMIC waves through cyclotron resonance according to Miyoshi et al. (2008).

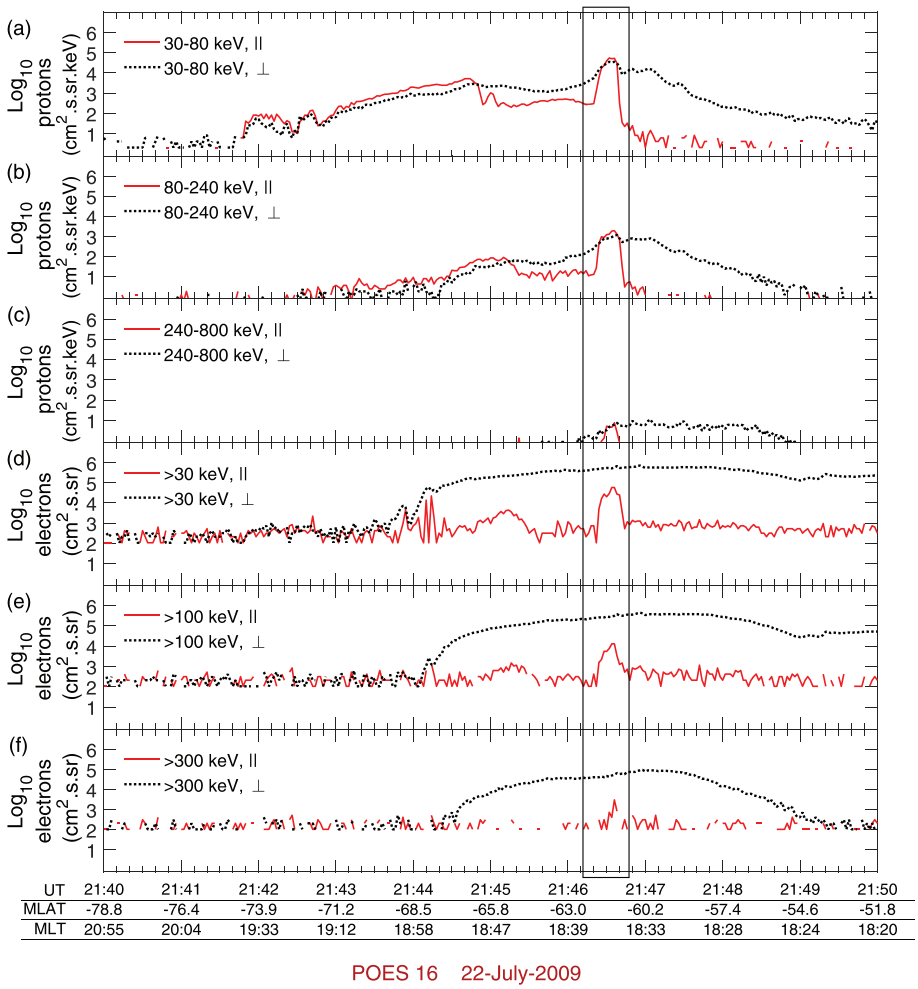

Figure 4. Particle measurements by POES-16 on 22 July 2009. (a) Protons with energies between 30 and 80 keV. (b) Protons with energies at 80–240 keV. (c) Protons with energies between 240 and 800 keV. (d) Electrons above 30 keV. (e) Electrons above 100 keV. (f) Electrons at energies above 300 keV. The red and black lines denote the particles observed by 0° and 90° telescopes, respectively. A black box shows the particle spectra at the locations where the subauroral isolated spots occurred.

4.2. Ion Precipitation Mechanism

Previous works have suggested that the energetic protons/ions related to isolated spots, isolated arc, and dayside detached auroras can be scattered by EMIC waves through a mechanism named cyclotron resonance (Yahnin et al., 2007; Sakaguchi et al., 2007; Ozaki et al., 2018; Zhou et al., 2018). The ion cyclotron instability is expected to produce both the growth of the EMIC waves and the scattering of energetic ions into the loss cone (Yahnin et al., 2007). EMIC waves are commonly enhanced under magnetic storm conditions as anisotropic energetic ring current ions are injected into the inner magnetosphere (Fraser et al., 2010; Jordanova et al., 2008). The group velocity of EMIC waves is nearly aligned with the magnetic field lines. Therefore, they can propagate to the Earth and can be observed in Pc1 and Pc2 bands (Engebretson et al., 2008). Figure 5c shows that the magnetometer at PINA station observed three Pc1 events during the duration of the isolated auroral spots. It is well known that the Pc1 geomagnetic pulsations at frequencies of ~1 Hz can propagate horizontally for more than 1,000 km through the ionospheric duct (Fraser, 1975; Jun et al., 2016). Yahnina et al. (2000) have suggested that the intense Pc1 on the ground can be observed at any distance (in MLT) from the location of the proton enhancement but the probability to catch the Pc1 pulsation strongly decreases with the distance. It is therefore expected that the temporal variation of the Pc1 pulsation observed at PINA in Figure 5c had an origin from the Pc1 in the magnetosphere, rather than the motion of the PINA station relative to the isolated spots. Figure 5c implies that the EMIC waves were not excited consecutively.

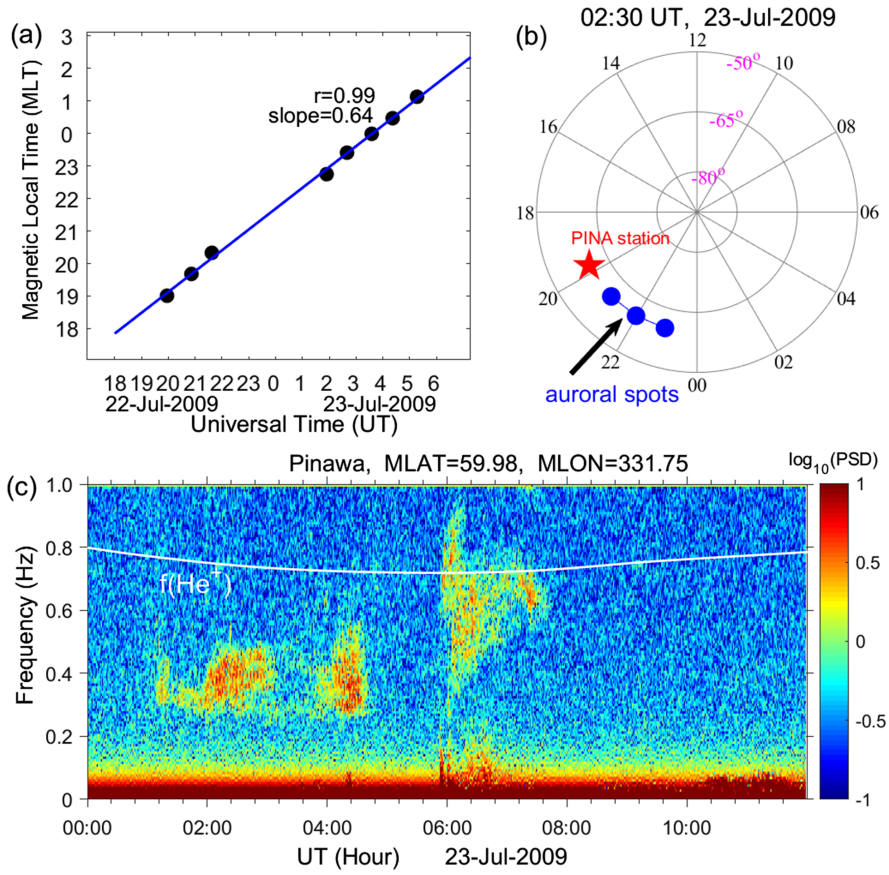

Figure 5. (a) Fitted line for the positions of the ECP. The nine black dots correspond to the eastside edge of the ECP shown in Figure 2. (b) The positions of PINA station and estimated ECP at 02:30 UT on 23 July 2009. The coordinate used in (b) is the same as Figure 2. (c) Pc1 (0–1 Hz) recorded by the magnetometer at PINA station between 00:00 UT and 12:00 UT on 23 July 2009. The white line in (c) shows the gyrofrequency of helium ion in the magnetic equatorial plane.

Instead, they appeared to be three wavelets which were separated by nearly one UT hour. This separation likely caused the auroral spots not being visible in Figures 2e and 2f.

4.3. Plasmapause Associated With the Isolated Auroral Spots

EMIC waves are commonly observed near the magnetopause when magnetic storms occur. We run a three-dimensional dynamic kinetic model of the plasmasphere to investigate the source region of the isolated spots. This model uses the kinetic approach to determine the moments of the particles inside the plasmasphere (Pierrard & Stegen, 2008). The position of the plasmapause is determined based on the interchange instability mechanism. The *Kp*-dependent empirical electric field model E5D (McIlwain, 1986) is used in the kinetic model to determine the convection velocity, and ultimately the position of the plasmapause. The plasmaspheric model is generalized in three dimensions by calculating the velocity distribution function along different flux tubes. By taking into account the corotation and the convection velocity depending on the *Kp* index, the model becomes dynamic (Pierrard & Stegen, 2008). Previous studies have shown a good consistency of the plasmapause position between the modeling and the observations of satellites (Pierrard & Stegen, 2008; Pierrard & Voiculescu, 2011; Verbanac et al., 2018; Yahnin et al., 2013). Figure 6 gives the position of the model predicted plasmapause around 21:30 UT on 22 July 2009. That is almost the same time as the isolated spots shown in Figure 2d. The isolated spots are mapped in the magnetic equatorial plane on the basis of T96 model (Tsyganenko, 1995). It is clearly seen in Figure 6 that the isolated spots are mapped in L shell between 4 and 6 at the equatorial plane, suggesting that the source region of the isolated spots is close to the plasmapause. The plasmasphere is presumed to consist of cold dense particles and overlaps with the

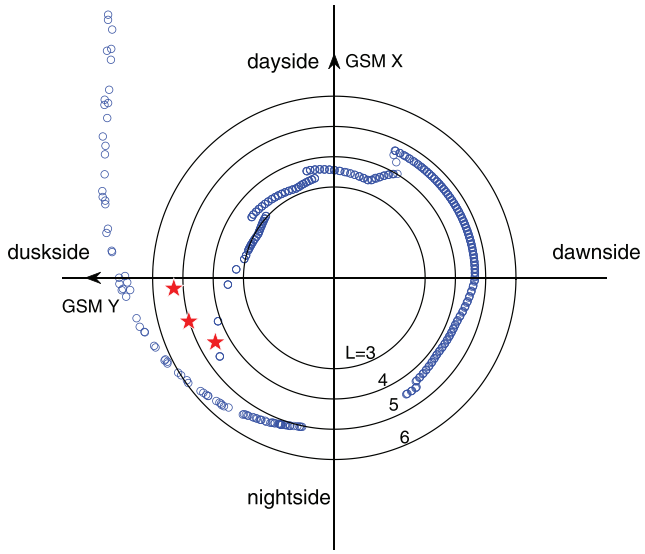

Figure 6. Modeled plasmapause (blue circle) and isolated spots (red stars) mapped onto the magnetic equatorial plan in GSM coordinate around 21:30 UT on 22 July 2009. The black lines indicate the L shell of 3, 4, 5, and 6, respectively.

ring current, which allows the growth rate of the EMIC waves to be amplified (Pickett et al., 2010; Thorne & Horne, 1992). It is expected that the EMIC waves can be cyclotron resonated with the energetic ions which precipitate into the ionosphere and can be observed by the DMSP and POES spacecraft. Yahnin et al. (2013) have indicated that often the proton aurora spot source was located in the vicinity of the plasmapause or in the cold plasma inside the plasmasphere. The proton aurora spots can be also well outside the plasmapause (Yahnin et al., 2013). Previous works also indicated that the wave-particle interactions between EMIC waves and energetic ions were account for subauroral proton spots (Yahnin et al., 2007), isolated proton arcs (Sakaguchi et al., 2007), isolated proton auroras (Miyoshi et al., 2008; Ozaki et al., 2018), and dayside detached auroras (Zhou et al., 2018). Therefore, the results of the present work further support the association between the isolated auroral spots, particle precipitations, plasmapause location, and Pc1 pulsations as reported by previous investigations (Sakaguchi et al., 2007; Yahnin et al., 2007; Miyoshi et al., 2008; Ozaki et al., 2018).

4.4. Precipitation of Energetic Electrons (30–300 keV)

Another mechanism, nonresonant interactions, can be an explanation for those precipitations of electrons having energies between 30 and 300 keV. Chen et al. (2016) suggested that the pitch angle scattering due to nonresonant interactions occurs often when the electrons encounter a sharp leading of EMIC wave packet. They suggested that the EMIC waves can cause significant pitch angle scattering for electrons with energies down to hundreds of keV, which is much lower than the minimum resonant energy required for the cyclotron resonance. The present work shows electrons with energies between 30 and 300 keV precipitating into the isolated auroral spots. The electron energy range and Pc1 occurrence are well consistent with the nonresonant interactions discussed by Chen et al. (2016).

4.5. The Isolated Auroral Spots Corotate With the Earth

As it is well known, the plasmasphere consists of cold and low-density plasma with energies of several eV (Singh et al., 2011). The plasmasphere corotates with the Earth under the action of the corotational electric field which points into the center of the Earth (Singh et al., 2011). The ionospheric disturbance dynamo was suggested to be the cause of the lag between the plasmasphere and the Earth (Burch et al., 2004). The isolated spots reported in this work corotate with 64% of the full speed of the Earth, which is slightly smaller than the 70%–95% corotation speed as reported by previous works (Burch et al., 2004; Frey et al., 2004). Moldwin et al. (1995) indicated that under moderate to high levels of geomagnetic activity conditions the outer plasmasphere typically had a fine-scale density structure on the order of 1,000 km or less. Previous works have suggested that the energetic precipitating particles are well correlated with the small-scale structures of the cold plasma or plasmaspheric tail (Yahnin et al., 2006). For the present work, Figure 6 indicates that the source region of the auroral spots is also located near to the plasmaspheric tail. The isolated auroral spots in the present work likely correspond to the plasmaspheric tail presumed to contain cold dense plasma. The corotational electric field is assumed to cause the cold plasma to transport through the $E \times B$ drift, leading the isolated auroral spots to corotate with the Earth. This explanation is also consistent with the IMF condition as shown in Figure 1. As shown during the period between the two vertical lines in Figure 1d, the auroral spots were observed when the IMF B_z changed to nearly zero. For this reason, the convection electric field likely decreased. It is therefore expected that the corotational electric field was going to be dominant, and led the dense cold plasma to corotate and move toward the evening sector.

5. Summary

The present work reports isolated auroral spots observed by the DMSP/SSUSI in the southern hemisphere between 22 and 23 July 2009. This work reveals some characteristics of the isolated auroral spots and gives reasonable explanations for their creation. The results can be summarized as follows:

1. The isolated auroral spots were found to occur in the southern hemisphere and rotated from ~18:00 to ~02:00 MLT. They were observed during the recovery phase of a moderate magnetic storm with a minimum *SYM-H* of −90 nT. The isolated auroral spots lasted for around 10 hr and moved approximately along 60° MLAT with 64% of the Earth's rotational speed.
2. The isolated auroral spots were produced predominantly by the precipitating ions with energies between 10 and 240 keV. These energetic ions were most likely dumped from the ring current presumed to be filled with hot ions during the recovery phase of a magnetic storm. Precipitation of energetic electrons at energies of 30–300 keV was also observed into these isolated auroral spots.
3. The magnetometer at ground station observed significant Pc1 pulsations, which correlated well with the occurrence time and location of the isolated auroral spots. The Pc1 likely originated from the EMIC waves excited in the magnetosphere. The present results indicate that the energetic ions associated with auroral spots are consistent with being scattered into the loss cone via EMIC waves.
4. Modeling result indicates that the isolated auroral spots are mapped to 4–6 L shell in the magnetic equatorial plane. This suggests that the source region for the isolated auroral spots is located in the vicinity of the plasmapause, which favors the amplification of the EMIC waves.

Acknowledgments
We would like to thank Johns Hopkins University Applied Physics Laboratory for providing the DMSP/SSUSI auroral FUV data (available at https://ssusi.jhuapl.edu/data_products) and DMSP/SSJ data (available at http://sd-www.jhuapl.edu/Aurora/). This work was supported by the Natural Science Foundation of China (41774174, 41874184, 41674154, and 41904139). We acknowledge use of NASA/GSFC's Space Physics Data Facility's OMNIWeb service, and OMNI data. The authors thank I.R. Mann, D.K. Milling, and the rest of the CARISMA team for data. CARISMA is operated by the University of Alberta, funded by the Canadian Space Agency.

References

Burch, J. L., Goldstein, J., & Sandel, B. R. (2004). Cause of plasmasphere corotation lag. *Geophysical Research Letters*, *31*, L05802. https://doi.org/10.1029/2003GL019164

Burch, J. L., Lewis, W. S., Immel, T. J., Anderson, P. C., Frey, H. U., Fuselier, S. A., et al. (2002). Interplanetary magnetic field control of afternoon-sector detached proton auroral arcs. *Journal of Geophysical Research*, *107*(A9), 1251. https://doi.org/10.1029/2001JA007554

Chen, L., Thorne, R. M., Bortnik, J., & Zhang, X.-J. (2016). Nonresonant interactions of electromagnetic ion cyclotron waves with relativistic electrons. *Journal of Geophysical Research: Space Physics*, *121*, 9913–9925. https://doi.org/10.1002/2016JA022813

Engebretson, M. J., Lessard, M. R., Bortnik, J., Green, J. C., Horne, R. B., Detrick, D. L., et al. (2008). Pc1–Pc2 waves and energetic particle precipitation during and after magnetic storms: Superposed epoch analysis and case studies. *Journal of Geophysical Research*, *113*, A01211. https://doi.org/10.1029/2007JA012362

Evans, D. S., & Greer, M. S. (2000). Polar orbiting environmental satellite space environment monitor-2: Instrument description and archive data documentation, Boulder, Colo. : U.S. Dept. of Commerce, National Oceanic and Atmospheric Administration, Oceanic and Atmospheric Research Laboratories, Space Environment Center.

Fraser, B. J. (1975). Ionospheric duct propagation and Pc 1 pulsation sources. *Journal of Geophysical Research*, *80*(19), 2790–2796. https://doi.org/10.1029/JA080i019p02790

Fraser, B. J., Grew, R. S., Morley, S. K., Green, J. C., Singer, H. J., Loto'aniu, T. M., & Thomsen, M. F. (2010). Storm time observations of electromagnetic ion cyclotron waves at geosynchronous orbit: GOES results. *Journal of Geophysical Research*, *115*, A05208. https://doi.org/10.1029/2009JA014516

Frey, H. U. (2007). Localized aurora beyond the auroral oval. *Reviews of Geophysics*, *45*(1), RG1003. https://doi.org/10.1029/2005RG000174.

Frey, H. U., Haerendel, G., Mende, S. B., Forrester, W. T., Immel, T. J., & Østgaard, N. (2004). Subauroral morning proton spots (SAMPS) as a result of plasmapause-ring-current interaction. *Journal of Geophysical Research*, *109*, A10305. https://doi.org/10.1029/2004JA010516

Hardy, D. A., L. K. Schmitt, M. S. Gussenhoven, F. J. Marshall, H. C. Yeh, T. L. Shumaker, et al. (1984), Precipitating electron and ion detectors (SSJ/4) for the block 5D/flights 6 – 10 DMSP satellites: Calibration and data presentation., Air Force Geophys. Lab., Hanscom Air Force Base, Bedford, Mass.

Immel, T. J., Mende, S. B., Frey, H. U., Peticolas, L. M., Carlson, C. W., Gérard, J.-C., et al. (2002). Precipitation of auroral protons in detached arcs. *Geophysical Research Letters*, *29*(11), 1519. https://doi.org/10.1029/2001GL013847

Jordanova, V. K., Albert, J., & Miyoshi, Y. (2008). Relativistic electron precipitation by EMIC waves from self-consistent global simulations. *Journal of Geophysical Research*, *113*, A00A10. https://doi.org/10.1029/2008JA013239

Jun, C.-W., Shiokawa, K., Connors, M., Schofield, I., Poddelsky, I., & Shevtsov, B. (2016). Possible generation mechanisms for Pc1 pearl structures in the ionosphere based on 6 years of ground observations in Canada, Russia, and Japan. *Journal of Geophysical Research: Space Physics*, *121*, 4409–4424. https://doi.org/10.1002/2015JA022123

King, J. H., & Papitashvili, N. E. (2005). Solar wind spatial scales in and comparisons of hourly Wind and ACE plasma and magnetic field data. *Journal of Geophysical Research*, *110*, A02104. https://doi.org/10.1029/2004JA010649

Kubota, M., Nagatsuma, T., & Murayama, Y. (2003). Evening co-rotating patches: A new type of aurora observed by high sensitivity all-sky cameras in Alaska. *Geophysical Research Letters*, *30*(12), 1612. https://doi.org/10.1029/2002GL016652

Mann, I. R., Milling, D. K., Rae, I. J., Ozeke, L. G., Kale, A., Kale, Z. C., et al. (2008). The Upgraded CARISMA Magnetometer Array in the THEMIS Era. *Space Science Reviews*, *141*(1-4), 413–451. https://doi.org/10.1007/s11214-008-9457-6

McIlwain, C. E. (1986). A Kp dependent equatorial electric field model. *Advances in Space Research*, *6*(3), 187–197. https://doi.org/10.1016/0273-1177(86)90331-5

Mendillo, M., Baumgardner, J., & Providakes, J. (1989). Ground-based imaging of detached arcs, ripples in the diffuse aurora, and patches of 6300-Å emission. *Journal of Geophysical Research*, *94*(A5), 5367–5381. https://doi.org/10.1029/JA094iA05p05367

Miyoshi, Y., Sakaguchi, K., Shiokawa, K., Evans, D., Albert, J., Connors, M., & Jordanova, V. (2008). Precipitation of radiation belt electrons by EMIC waves, observed from ground and space. *Geophysical Research Letters*, *35*, L23101. https://doi.org/10.1029/2008GL035727

Moldwin, M. B., Thomsen, M. F., Bame, S. J., McComas, D., & Reeves, G. D. (1995). The fine-scale structure of the outer plasmasphere. *Journal of Geophysical Research*, *100*(A5), 8021–8029. https://doi.org/10.1029/94JA03342

Moshupi, M. C., Anger, C. D., Murphree, J. S., Wallis, D. D., Whitteker, J. H., & Brace, L. H. (1979). Characteristics of trough region auroral patches and detached arcs observed by Isis 2. *Journal of Geophysical Research*, *84*(A4), 1333–1346. https://doi.org/10.1029/JA084iA04p01333

Ozaki, M., Shiokawa, K., Miyoshi, Y., Kataoka, R., Connors, M., Inoue, T., et al. (2018). Discovery of 1 Hz Range Modulation of Isolated Proton Aurora at Subauroral Latitudes. *Geophysical Research Letters*, *45*, 1209–1217. https://doi.org/10.1002/2017GL076486

Paxton, L. J., Morrison, D., Zhang, Y., Kil, H., Wolven, B., Ogorzalek, B. S., et al. (2002). Validation of remote sensing products produced by the Special Sensor Ultraviolet Scanning Imager (SSUSI): a far UV-imaging spectrograph on DMSP F-16.

Pickett, J. S., Grison, B., Omura, Y., Engebretson, M. J., Dandouras, I., Masson, A., et al. (2010). Cluster observations of EMIC triggered emissions in association with Pc1 waves near Earth's plasmapause. *Geophysical Research Letters*, *37*, L09104. https://doi.org/10.1029/2010GL042648

Pierrard, V., & Stegen, K. (2008). A three-dimensional dynamic kinetic model of the plasmasphere. *Journal of Geophysical Research*, *113*, A10209. https://doi.org/10.1029/2008JA013060

Pierrard, V., & Voiculescu, M. (2011). The 3D model of the plasmasphere coupled to the ionosphere. *Geophysical Research Letters*, *38*, L12104. https://doi.org/10.1029/2011GL047767

Redmon, R. J., Denig, W. F., Kilcommons, L. M., & Knipp, D. J. (2017). New DMSP database of precipitating auroral electrons and ions. *Journal of Geophysical Research: Space Physics*, *122*, 9056–9067. https://doi.org/10.1002/2016JA023339

Sakaguchi, K., Shiokawa, K., Ieda, A., Miyoshi, Y., Otsuka, Y., Ogawa, T., et al. (2007). Simultaneous ground and satellite observations of an isolated proton arc at subauroral latitudes. *Journal of Geophysical Research*, *112*, A04202. https://doi.org/10.1029/2006JA012135

Sakaguchi, K., Shiokawa, K., Miyoshi, Y., Otsuka, Y., Ogawa, T., Asamura, K., & Connors, M. (2008). Simultaneous appearance of isolated auroral arcs and Pc 1 geomagnetic pulsations at subauroral latitudes. *Journal of Geophysical Research*, *113*, A05201. https://doi.org/10.1029/2007JA012888

Singh, A. K., Singh, R. P., & Siingh, D. (2011). State studies of Earth's plasmasphere: A review. *Planetary and Space Science*, *59*(9), 810–834. https://doi.org/10.1016/j.pss.2011.03.013

Sotirelis, T., Korth, H., Hsieh, S.-Y., Zhang, Y., Morrison, D., & Paxton, L. (2013). Empirical relationship between electron precipitation and far-ultraviolet auroral emissions from DMSP observations. *Journal of Geophysical Research: Space Physics*, *118*, 1203–1209. https://doi.org/10.1002/JGRA.50157

Spasojević, M., Frey, H. U., Thomsen, M. F., Fuselier, S. A., Gary, S. P., Sandel, B. R., & Inan, U. S. (2004). The link between a detached subauroral proton arc and a plasmaspheric plume. *Geophysical Research Letters*, *31*, L04803. https://doi.org/10.1029/2003GL018389

Thorne, R. M., & Horne, R. B. (1992). The contribution of ion-cyclotron waves to electron heating and SAR-arc excitation near the storm-time plasmapause. *Geophysical Research Letters*, *19*(4), 417–420. https://doi.org/10.1029/92GL00089

Tsyganenko, N. A. (1995). Modeling the Earth's magnetospheric magnetic field confined within a realistic magnetopause. *Journal of Geophysical Research*, *100*(A4), 5599–5612. https://doi.org/10.1029/94JA03193

Verbanac, G., Bandić, M., Pierrard, V., & Cho, J. (2018). MLT Plasmapause Characteristics: Comparison Between THEMIS Observations and Numerical Simulations. *Journal of Geophysical Research: Space Physics*, *123*, 2000–2017. https://doi.org/10.1002/2017JA024573

Yahnin, A. G., Yahnina, T. A., & Demekhov, A. G. (2006). Interrelation between localized energetic particle precipita ion and cold plasma inhomogeneities in the magnetosphere. *Geomagnetism and Aeronomy*, *46*(3), 332–338. https://doi.org/10.1134/s0016793206030078

Yahnin, A. G., Yahnina, T. A., Frey, H., & Pierrard, V. (2013). Sub-oval proton aurora spots: Mapping relatively to the plasmapause. *Journal of Atmospheric and Solar-Terrestrial Physics*, *99*, 61–66. https://doi.org/10.1016/j.jastp.2012.09.018

Yahnin, A. G., Yahnina, T. A., & Frey, H. U. (2007). Subauroral proton spots visualize the Pc1 source. *Journal of Geophysical Research*, *112*, A10223. https://doi.org/10.1029/2007JA012501

Yahnina, T. A., Yahnin, A. G., Kangas, J., & Manninen, J. (2000). Proton precipitation related to Pcl pulsations. *Geophysical Research Letters*, *27*(21), 3575–3578. https://doi.org/10.1029/2000GL003763

Yuan, Z., Deng, X., Lin, X., Pang, Y., Zhou, M., Décréau, P. M. E., et al. (2010). Link between EMIC waves in a plasmaspheric plume and a detached sub-auroral proton arc with observations of Cluster and IMAGE satellites. *Geophysical Research Letters*, *37*, L07108. https://doi.org/10.1029/2010GL042711

Zhang, Y., Paxton, L. J., Morrison, D., Wolven, B., Kil, H., & Wing, S. (2005). Nightside detached auroras due to precipitating protons/ions during intense magnetic storms. *Journal of Geophysical Research*, *110*, A02206. https://doi.org/10.1029/2004JA010498

Zhou, S., Luan, X., Søraas, F., Østgaard, N., & Raita, T. (2018). The detached auroras induced by the solar wind pressure enhancement in both hemispheres from imaging and in situ particle observations. *Journal of Geophysical Research: Space Physics*, *123*, 3170–3182. https://doi.org/10.1002/2017JA024562